Motorcycle chassis design: frame development for the PreMoto3 motorcycle

Anders Mateusz[1], Dagiel Arkadiusz[2], and Skawinski Piotr[3]

[1, 2, 3] *Warsaw University of Technology, Faculty of Automotive and Construction Machinery Engineering, Poland*

Abstract.

The proper chassis design is crucial for success in motorcycle racing series, especially in those that require identical engines. The presented information is based on the process of developing the chassis for the PreMoto3 motorcycle prepared for the MotoStudent and MotoEngineering Cup competitions. Leading solutions made of materials such as steel and aluminium alloys demand a different approach in both, the element design process and the manufacturing process. The chosen approach has an impact on rigidity. It also provides a different possibility to manipulate the chassis flexure. The differences in structure stiffness are shown using the Finite Element Method. Several possible chassis configurations have been compared, including the design with several areas reinforced using Carbon Fibre Reinforced Polymer (CFRP) and with the additional stiffening element mounted. Furthermore, beam and shell FEM models of triangulated frames were also compared. The process of making a truss steel frame in unit production and the manufacturing process of a twin spar frame (based on aluminium alloys) were described. Amendments between the manufacturing process of trellis and beam frame were made based on the experience gained during truss frame manufacturing.

Keywords: motorcycle, chassis, FEA, manufacturing

1. Introduction and Objectives

The frame of the motorcycle is the main and crucial component of the whole chassis. It has to provide adequate driving characteristics (proper geometry and stiffness) while maintaining enough strength, both static and fatigue. Besides this, the chassis integrates other motorcycle parts, so its design must allow assembly of them. In the case of road motorcycles as well as the racing ones, chassis configuration cannot obstruct basic service maintenance. This article concerns the evolution of PreMoto3 motorcycle chassis, which has been developed following the rules of academic competitions, the MotoStudent, and the MotoEngineering Cup. Those motorcycles are all equipped with the same 250 cm3 single-cylinder engines. The minimal weight of the vehicle is limited to 95kg. Similar engine power and low vehicle mass (compared to road motorcycles) challenge the design process of each element. Each part must provide enough stiffness and strength while keeping the weight as low as possible. In the article, the design and manufacturing process of the triangulated frame, used in racing conditions in 2019 and 2020 were described. Also, a process of the redesign of the chassis to the new twin spar

frame was presented. Differences between both frames in stiffness and strength were pointed out using the Finite Element Method.

Figure 1: PreMoto3 motorcycle developed by WSRT Engineering

The role of the frame is to ensure the proper traction capabilities of the vehicle. Besides, this part integrates all components of the motorcycle. It must connect the headstock and the swingarm pivot while reaching the rigidity assumptions. Nowadays, in racing two solutions are under consideration: triangulated and twin spar frames. Triangulated frames can have extremely high structural efficiency. They are manufactured using tubes (mostly steel) welded in a manner that meets the requirements of the correct triangulation. Factories gradually abandon the solution, because of the complexity and the hard effort needed for automation of this manufacturing process. Anyway, it is popular among prototype motorcycles due to the relatively low cost of unit production. The triangulated chassis is suitable for narrow, single-cylinder or V-twin engines, for which the frame structure is relatively simple. An example of a complex triangulated frame designed for a wide inline four-cylinder engine in Moto2 class (which development was stopped after three seasons) is shown in Fig. 2. Despite these shortcomings, the design process is relatively simple, so it allows engineers to prepare several solutions in short interval, with different flexure characteristics.

Figure 2 : Triangulated frame: a) example of correct triangulation, b) complex KTM Moto2 frame for 4-inline cylinder engine

Example of correct triangulation
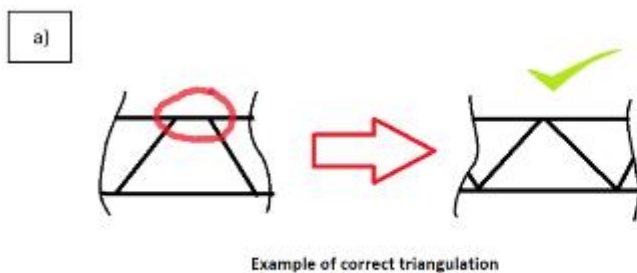
Source: a) MotoStudent Competition Regulations, b) www.drivetribe.com

The shape and the size of the modern inline three or four-cylinder engines, and complicated manufacturing process were the main reasons, why trellis frames have been replaced with twin spar frames made of aluminium alloys. In this solution headstock and swingarm pivot are connected with two beams running each side of the engine. Side members are typically made by extruding, fabrication from sheets, or casting (Foale, 2002). The production of racing chassis requires milling components out of aluminium blocks (Fig. 3). The number of elements is significantly reduced. It allows the simplification of the production process. Besides this, the twin spar frame has packaging advantages, especially for modern motorcycles with large air-boxes and wide engines. With more freedom during the design phase, it is possible to style the shape of the frame to enhance maintenance care works, for example, spark plugs replacement. On the other hand, the design process is much more complicated. However, as will be presented later, the beam frames allow more control of the chassis flexibility.

Figure 3: Prototype beam frames: a) example of milled main beam, b) KalexMoto2 beam frame
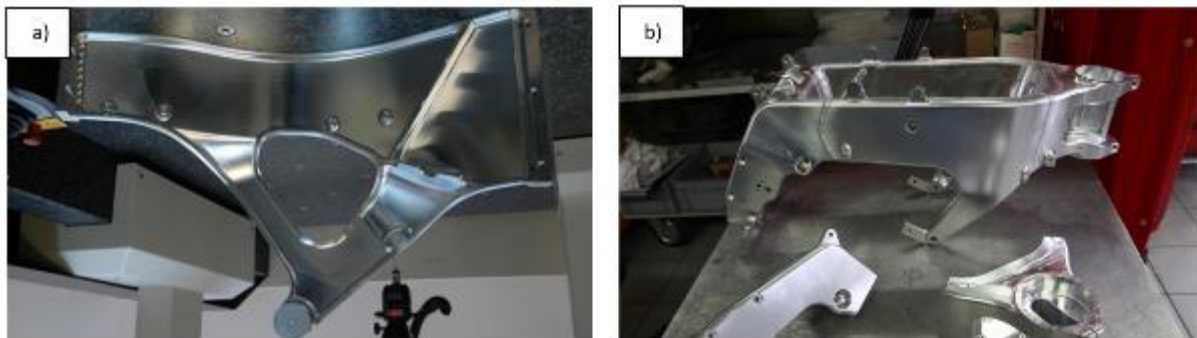
Source: a) www.dr-moto-co.uk, b) www.blog.ktm.com

The structural stiffness of the frame and other chassis components have a significant impact on damping of the structural vibrations excited in motion, especially weave and wobble mode. The weave mode is characterized by sizable oscillations in roll, yaw, and steering angle. The wobble one, in turn, as rotations of the front part of the frame while the rear one is relatively stable (Cossalter, 2006). The torsional flexibility of the upper part near the headstock with the lateral flexibility of the front fork stabilizes the wobble mode at high speeds and has the contrary effect at low velocity. The lateral flexibility of the rear frame or swingarm has an positive impact on stabilizing the weave mode when the torsional flexibility of both has an opposite effect. As (Cossalter, 2006) says, over some values of the torsional and the lateral stiffness of the frame, motorcycle stability is only slightly dependant on the structural stiffness. High stiffness provides precise handling and rapid response to driver actions, while at the same time causing nervous handling on a bumpy surface or obstruct driving on low friction surfaces (for example wet road). As a result, road motorcycle frames have more flexibility, both torsional and lateral, than those designed for racing. Chassis should have moderate lateral stiffness and high torsional stiffness for the proper vibrations damping (Cossalter, 2006). Moderate values of lateral stiffness are also desired in terms of the front wheel grip. While going straight, forces from surface irregularities act in the plane of movement of the suspension.

When a bike is inclined, the plane of the movement of the suspension is no longer parallel to the direction of the forces caused by surface imperfections. The increased lateral stiffness of the chassis adds load on the tire (irregularities absorbed by the tire deflection rather than a suspension movement and front frame lateral deflection), which is already loaded by the lateral force. It can cause a lower speed in corner apex or even tire skid. As a result, lateral flexibility should be maintained in a specific optimal range, not necessarily as high as possible.

2. Methodology

2.1 Experimental testing

Chassis structural parameters are measured during bench tests on dedicated test rings (Fig. 4). The measurement of torsional stiffness is usually carried out together with the engine fitted, because the engine has a strong influence in overall structural stiffness of the chassis. For a frame locked at the swingarm pivot, a moment is applied to the steering head in an axis perpendicular to the axis of the steering head. Stiffness is defined as the ratio of the applied moment M_{φ} to the steering axis rotation φ (Eq. 1):

$$K_{\varphi} = \frac{M_{\varphi}}{\varphi} \left[\frac{Nm}{deg} \right] \tag{1}$$

During a flexural test, force is applied to the steering head when the pivot axis of the swingarm is locked. Lateral stiffness is defined as the ratio of the lateral force F and lateral displacement Δl measured in that direction (Eq. 2):

$$K_l = \frac{F}{\Delta l} \left[\frac{N}{mm} \right] \tag{2}$$

In order to facilitate the analysis of the results, the lateral force should be applied to the point located on the extension of the steering head axis, for which we do not observe torsional deformation.

Figure 4: Example of test rig
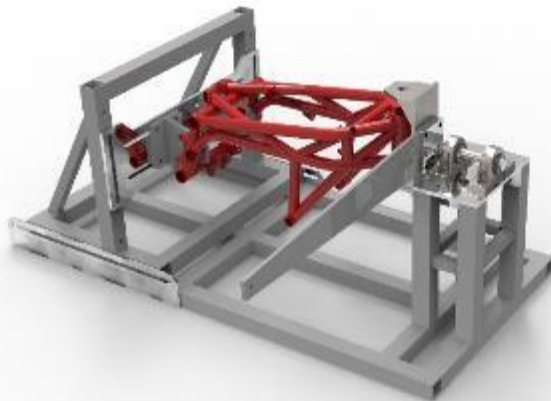
Unfortunately, in the literature, there is a lack of information about structural stiffness values of already produced chassis. Some of the values have been collected in Tab. 1.

Table 1: Typical values of torsional and lateral stiffness of motorcycle frames, engine fitted

Motorcycle Type	Type	Value
Modern 1000c bikes [1]	torsional	3 – 7 kNm/deg
Modern 1000c bikes [1]	lateral	1 – 3 kN/mm
Supermoto frame example [2]	torsional	1,32 kNm/deg

Source: [1] (Cossalter, 2006), [2] (Bocciolone et al., 2015)

2.2 Numerical Approach

During the development of the chassis for the 2019 season, in the first step simplified FEM calculations using beam elements have been used. All designs described below are based on identical chassis geometry as well as the position of the engine and rear suspension mounting points. Proposed constructions are shown in Fig. 5. They differ in the number of tubes and their configuration. All supporting tubes and all main ones have the same diameters and thickness. Torsional and lateral stiffness values are collected in Tab. 2. Preliminary calculations showed that the increase in torsional stiffness is associated with a significant increase in lateral stiffness, which makes it hard to meet the assumptions set out in the previous chapter. In the end, design No. 1 has been selected due to the highest stiffness-to-weight ratio.

Figure 5: Layout of triangulated frames for WSRT PreMoto3 2019 motorcycle
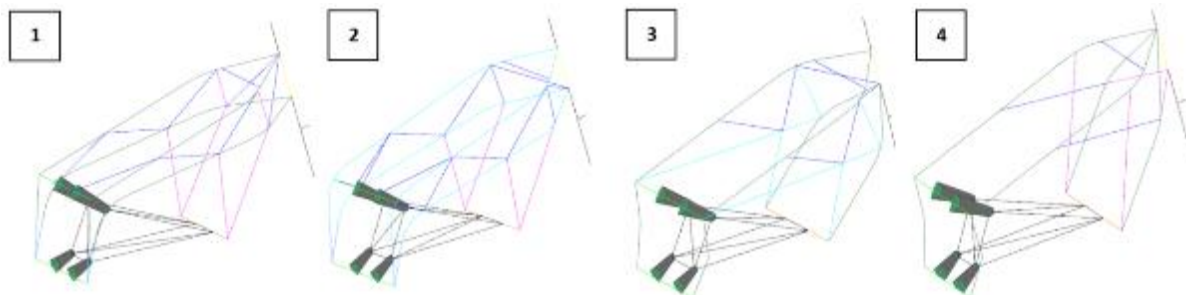
Table 2: Triangulated frames stiffness comparison (beam FE model)

	Torsional stiffness K_φ	$K_\varphi/mass$ ratio	Lateral stiffness K_l	$K_l/mass$ ratio
	Nm/deg	$Nm/(deg \cdot kg)$	N/mm	$N/(mm \cdot kg)$
Design 1	3228	449	2174	302
Design 2	2532	355	2041	206
Design 3	2740	393	1087	156
Design 4	2534	444	971	170

Development frame for 2021 shown in Fig. 6 is a twin spar chassis made of aluminium alloys.

Figure 6: Frame design: a) triangulated frame for 2019 bike, b) twin spar frame for ver. 2021
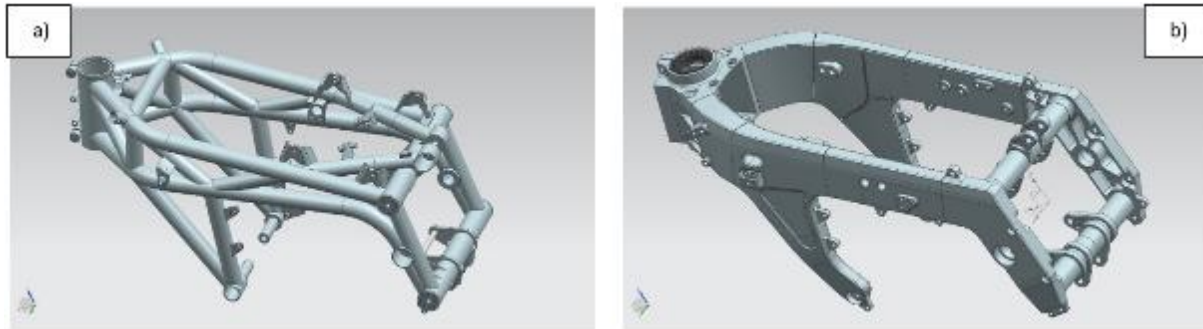
Both the CAD models of the 2019 and 2021 frames needed to be adapted for numerical calculations. Due to the complexity, the example of the twin spar chassis is described:

1. Main beams running around the engine modeled as shell elements (A) (Fig. 7). Headstock (B), suspension and engine fixing points (C), as well as side plates (D) modeled as solid elements discretized using Hex Dominant method.
2. Engine represented as a beam structure between the engine fixing points (Fig. 8a). Assuming that the engine is a rigid element compared to the stiffness of the frame, the beams have been assigned material with two orders of magnitude larger Young's modulus.
3. Ribs in the main beams have been modelled as surface elements (Fig. 8b).
4. The surface element (B in Fig. 7) passing through the headstock has been introduced. It allowed the correct transformation of various loads (e.g. forces at the tire-road contact patch used in strength calculations) to the whole structure.

Figure 7. FEA model discretization
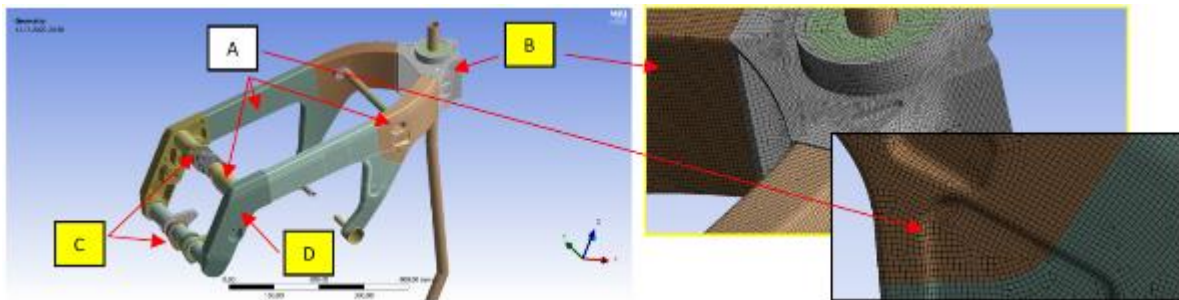
Figure 8: Simplification for FEA analysis
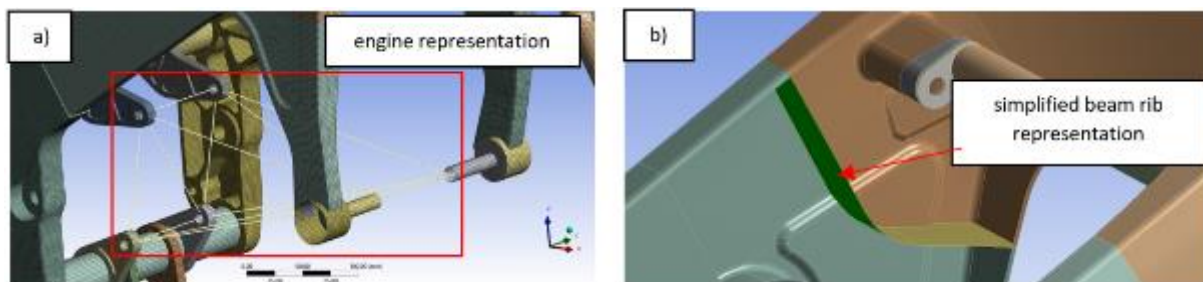
All degrees of freedom for the surface of the swingarm pivot (Fig. 9) has been received, so it was possible to represent real torsional stiffness test conditions correctly. In the real test, the loading arm rotates around an axis perpendicular to the axis of the steering head at its central point. The cylindrical support boundary condition for free rotation of the virtual loading arm is assigned to surface B – Fig. 7.

Figure 9: Boundary conditions for torsional stiffness test
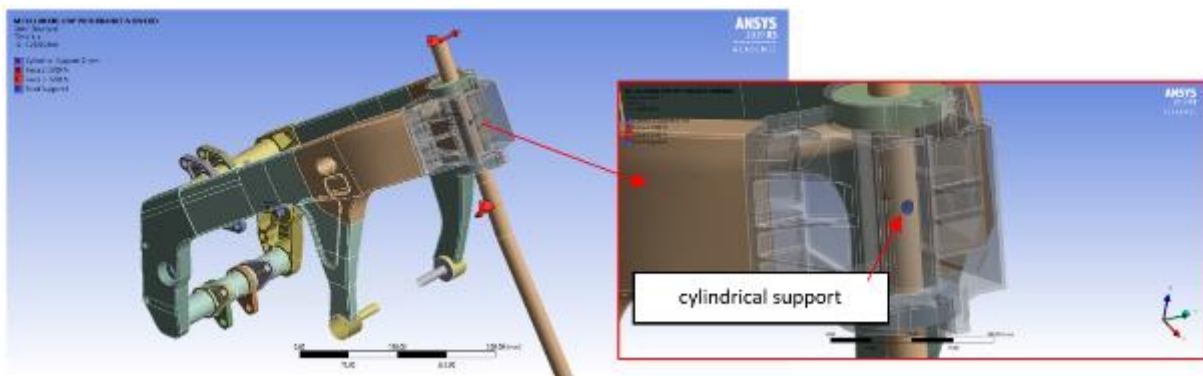
For the lateral stiffness test, the only boundary condition is the fixed support boundary for the swingarm pivot. A force of 1000N has been applied at an iteratively selected point on the extension of the axis of the frame head, for a point in which we do not observe torsional deformation (Fig. 10). The results for triangulated and twin spar frames are included in Tab. 3.

Figure 10: Boundary conditions for flexural test
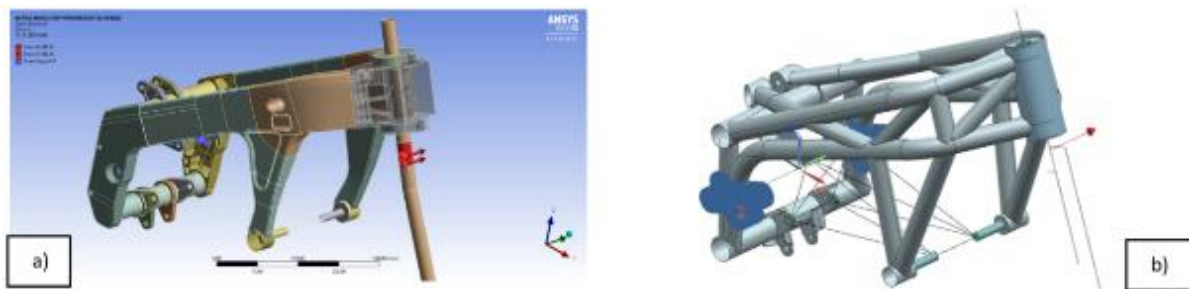
Table 3: Triangulated and twin spar frame comparison

	Torsional stiffness K_φ	$K_\varphi/mass$ ratio	Lateral stiffness K_l	$K_l/mass$ ratio
	Nm/deg	$Nm/(deg \cdot kg)$	N/mm	$N/(mm \cdot kg)$
Steel trellis frame (shell model)	$4098 \frac{Nm}{deg}$	$480.87 \frac{Nm}{kg \cdot deg}$	$2174 \frac{N}{mm}$	$255.10 \frac{N}{kg \cdot mm}$
Aluminium alloy twin spar	$3869.0 \frac{Nm}{deg}$	$601.61 \frac{Nm}{kg \cdot deg}$	$1492.5 \frac{N}{mm}$	$232.08 \frac{N}{kg \cdot mm}$

3. FEA Results Discussion

The developed twin spar frame is lighter by approximately 2 kg compared to the steel chassis while maintaining almost identical torsional stiffness. At the same time, lateral stiffness has been reduced to the level below 1.5 kN/mm, which is the lower range of values given by (Cossalter, 2006). The use of beams with cross-sections close to rectangular allows for greater freedom of managing flexibility. The twin spar frame design allows reducing lateral stiffness while maintaining torsional stiffness as for a steel chassis designed in 2019. Further reduction of lateral stiffness (if desired) can be achieved by changing the main beams cross-section thickness, or by narrowing the beams in the vertical direction near the connection area with the side plates containing the swingarm pivot. Examples of FE results are presented in Fig. 11.

Figure 11: FE results for torsion test
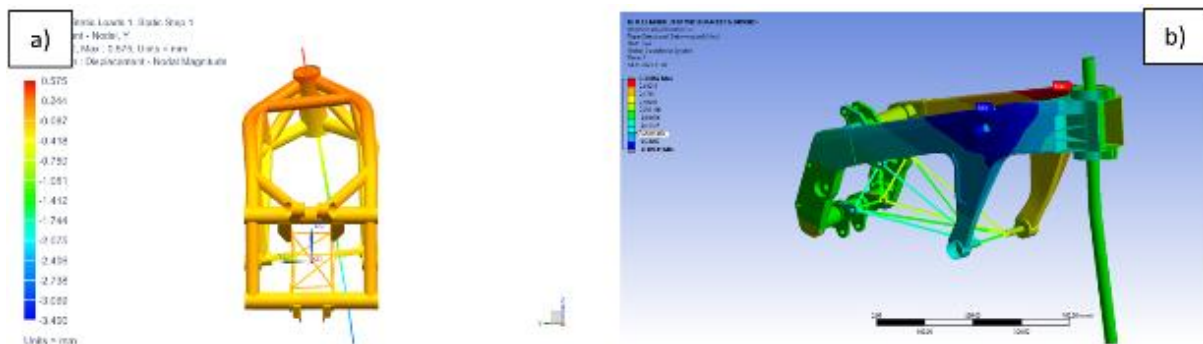
When reviewing the results of the beam and shell FEM models for the triangulated frame, an underestimation of the torsional stiffness value for the beam model and a very good correlation of lateral stiffness are noticeable. Differences in torsional stiffness values between the beam and shell model may arise from the simplified model of engine fixing points in the beam model and to the fact that the geometric representation of frame nodes in the shell model is much stiffer but closer to reality. Stress values in stiffness tests are shown in Fig. 12. Taking into account the strength of the developed steel and aluminium alloy chassis, it was possible to increase the safety factors for the loads occurring during movement, despite the lower weight of the aluminium alloy chassis.

Figure 12: Von Mises stress: a) torsion test, b) flexural test
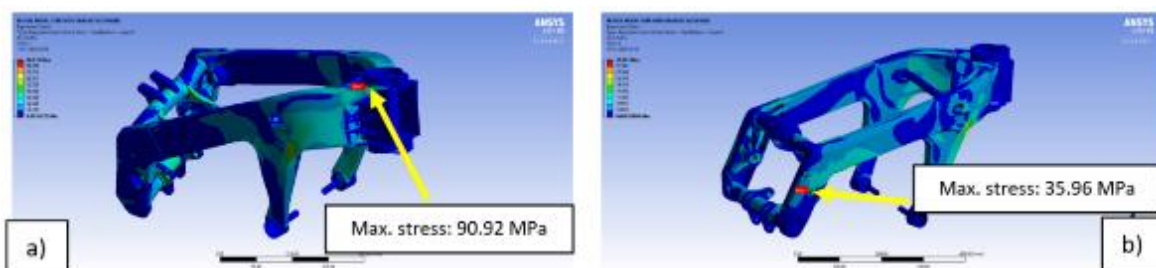
The frame design allows strengthening selected areas of the main beams using CFRP (Carbon Fibre Reinforced Polymer). To accommodate the new task conditions, the FEM model was decomposed in an ANSYS Workbench environment into blocks containing individual frame

elements, which later allowed the use of the ANSYS Composite PrePost module dedicated for laminated elements. For areas highlighted in Fig. 13a, a hybrid composite was defined as:

- base material: aluminium alloy PA45,
- woven prepreg in [45/-45] stacking sequence.

The individual modules containing subassemblies of the frame were then combined into one Static Structural analysis model.

Figure 13: The use of CFRP for chassis tuning
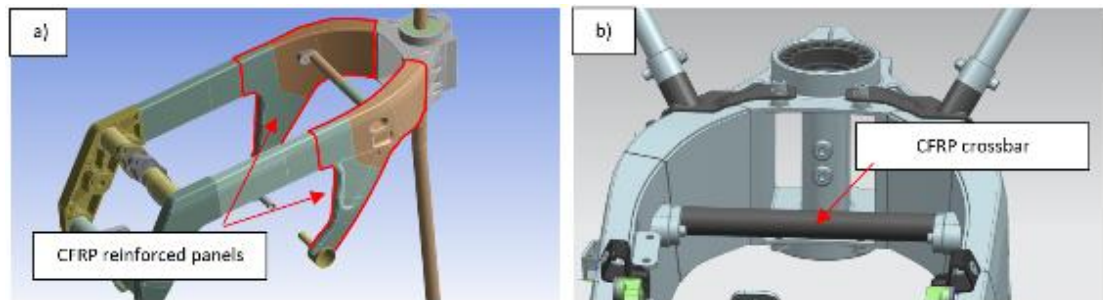
In addition, the newly developed frame can be tuned using the composite crossbar, which can be mounted in the front part of the frame (Fig. 13). The CFRP tube was modelled using the Composite PrePost module, adopting typical material values for woven, prepreg fabrics with layer sequence $[(45/-45)_2/45]_s$, where *s* is symmetric laminate. The results for the different configurations of the twin spar chassis are collected in Tab. 4.

Table 4: Possible configurations of twin spar frame: results comparison

	Torsional stiffness K_φ	$K_\varphi/mass$ ratio	Lateral stiffness K_l	$K_l/mass$ ratio
	Nm/deg	$Nm/(deg \cdot kg)$	N/mm	$N/(mm \cdot kg)$
Aluminium alloy	3869.0	601.61	1492.5	232.08
Aluminium alloy with CFRP crossbar	3894.6	599.26	1519.8	233.84
Carbon reinforced panels	4048.5	620.26	1567.4	240.14
Carbon reinforced panels with CFRP crossbar	4069.4	617.05	1592.4	241.45

Fig. 14 shows the percentage change in torsional and lateral stiffness for the beam frame for all cases (when identical values, coefficient assumes value 100%).

Figure 14: Torsional and lateral stiffness comparison

	Aluminium alloy	Aluminium alloy + crossbar	CFRP	CFRP + crossbar
Aluminium alloy	100.00%	99.34%	95.57%	95.07%
Aluminium alloy + crossbar	100.66%	100.00%	96.20%	95.70%
CFRP	104.64%	103.95%	100.00%	99.48%
CFRP + crossbar	105.18%	104.49%	100.52%	100.00%

Torsional stiffness comparison

	Aluminium alloy	Aluminium alloy + crossbar	CFRP	CFRP + crossbar
Aluminium alloy	100.00%	98.21%	95.22%	93.73%
Aluminium alloy + crossbar	101.82%	100.00%	96.96%	95.44%
CFRP	105.02%	103.13%	100.00%	98.43%
CFRP + crossbar	106.69%	104.78%	101.59%	100.00%

Lateral stiffness comparison

Considering all results, the twins spar design with the CFRP reinforced aluminium panels and the crossbar mounted has the highest torsional and lateral stiffness. Torsional stiffness to weight ratio takes the highest value for the composite reinforced frame, but without the crossbar mounted. The addition of two layers of carbon fibre for the aforementioned areas increases torsional stiffness by 4.64% and lateral stiffness by 5.02%. The effect of the crossbar on torsional stiffness is small, 0.66% for an aluminium alloy frame and 0.52% for a composite reinforced frame. The change in lateral stiffness is already more noticeable, 1.82% for the torsional stiffness of the aluminium alloy frame and 1.59% for the CFRP reinforced frame. The reinforcement process using woven prepregs can be performed at any time during the life cycle

of the frame, which gives the possibility to change the possible weakness of the chassis related to its stiffness.

4. Manufacturing Process Findings

The triangulated frame was made at the turn of 2018/2019. In the prepared project for budgetary reasons the use of milling operations was minimized, so all the frame components were made in processes such as: turning, laser cutting and bending on CNC bending machines. The use of CAD modelling allowed precise tube cutting. To produce the frame, a welding jig (Fig. 15) was designed. Laser-cut plates were used as positioning elements (A), which were located on the outside of the welding jig, attached to the base of the welding jig via wide angles (B). The position of the headstock was determined by a handle (C) which allowed the angular setting. Other component's position, in the perpendicular direction to the axis of symmetry of the frame, such as engine and suspension fixing points, was determined by threaded rods and sleeves.

Figure 15: Welding jig: The CAD model and a photo from the manufacturing process
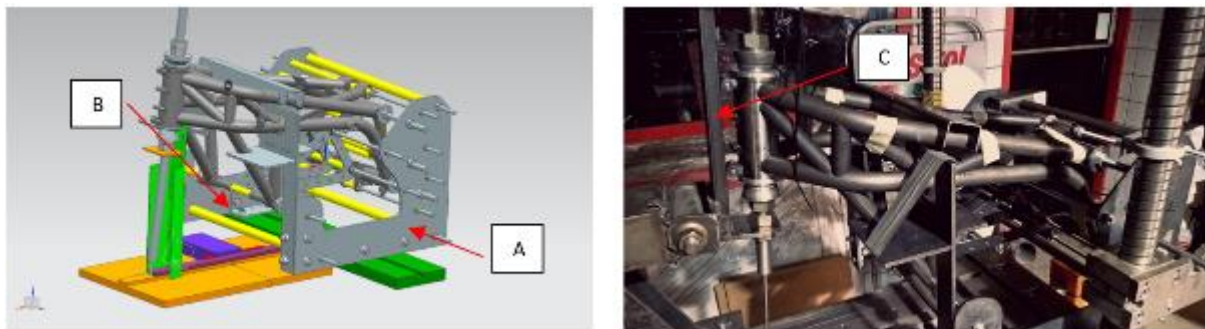
Precise laser cutting of tubing allowed to secure their position without additional tooling. The welding process was carried out using the TIG method using ER-70 wires. Used ER-70s welding wires for tube thickness, which is below 3mm, avoid the need for heat treatment after welding (Khaled, 2014).

The implemented process emphasized several problems, which might impede usage. That was because of errors in the manufacturing process and the specificities of triangulated frames:

1. Assembly process was time-consuming, due to two independent modules (headstock and the rear frame part) which required positioning using numerous elements.
2. Plates located outside the welded frame do not provide enough rigidity of the welding jig, so welding of aluminium alloys could lead to deformation that cannot be compensated at a later stage.
3. To reduce costs, elements such as the headstock were made in proper tolerance before the welding process. Welding stresses resulted in a slight local buckling. Furthermore, penetration of the weld inside the frame head was found, which prevented the installation of an insert containing headstock bearings without post-machining.
4. Heat treatment possible only for frame taken out from the welding jig, due to the large weight and dimensions of the jig.
5. Plates located on the outside of the welding frame impeded the welder's work.

With experience gained, several design changes have been made to the twin spar frame welding jig (Fig. 16). The welding jig was based on a central profile (A) with cross-section dimensions 100 x 80 x 4 mm. Fewer frame components allow the use of a simplified jig with supporting elements located inside the chassis. Frame parts have form-locking connections for easy positioning (C). The entire jig was based on the profiles and spacers. The use of threaded rods has been abandoned in favour of double end threaded studs machined from precision cold drawn rods.

Welding of the frame in its natural position has been left because it would be necessary to make a complex steering-head fixture placed at the proper angle. In the proposed solution, the frame headstock is bolted to the top surface of the main profile of the welding jig (B), so the difficulties related to the precise measurement of the steering head axis inclination can be avoided. Full access to welded joints (crucial for TIG welding) enables the cylindrical connection between the welding jig and the stand. Besides, the new design allows removing the jig (with the welded frame) from the stand, so heat treatment can be done for the whole assembly. To reduce the likelihood of distortion of tolerated surfaces, these were moved at the design stage away from the areas where the welds would be located.

Figure 16: Redesigned welding jig for twin spar aluminium alloy frame
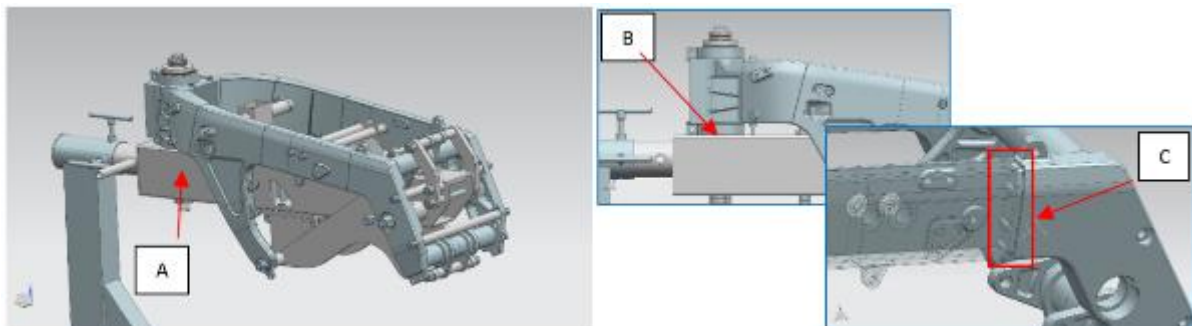
Typically, machining of allowances requires a 5-axis machining centre and additional tooling. To eliminate the inaccuracies created during welding, properly machined inserts can be mounted into the headstock and the swingarm pivot, thanks to which it is possible to remove minor deviations (Fig. 17). Moreover, inserts allow changing the geometrical parameters of the motorcycle, such as the caster angle and the position of the swingarm axis. Furthermore, they provide the possibility of the chassis set-up tune depending on the condition of the surface, track layout, and speed, as well as weather conditions.

Figure 17: Steering head and swingarm pivot inserts for axis offsetting
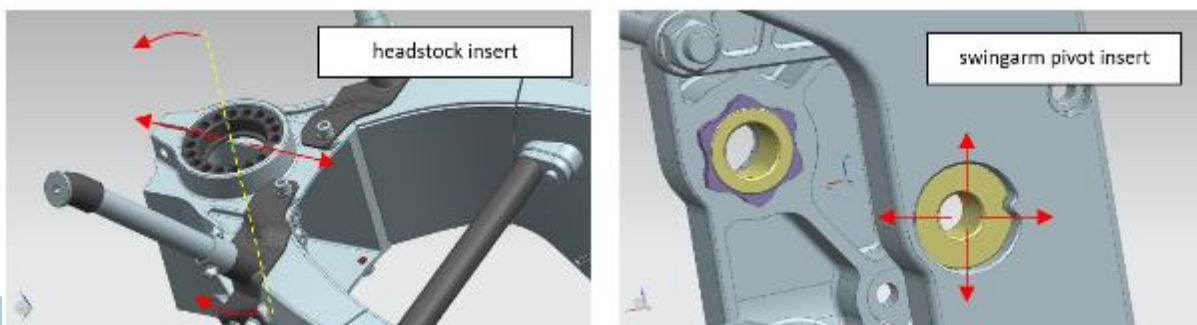
5. Conclusion

Comparison of the design and manufacturing process of the triangulated and twin spar frame for lightweight PreMoto3 motorcycle was highlighted. The requirements for assessing the structural efficiency of the chassis, the method of testing, and the applied loads have been laid down. The results for both types of frames are compiled and describes the differences in stiffness shaping capabilities. For the triangulated frame, as the truss structure is expanded, a significant increase in torsional and transverse stiffness is noticeable. The ability to control torsional stiffness when the lateral stiffness is strained at the desired level is limited. Too high lateral stiffness results in increased tire load for large lean angles, when the front suspension cannot work properly. The prototype twin spar beam frame based on milled elements allows for a wider possibility of chassis stiffness design by much larger possibility of selecting cross-sections of beams, changing the thickness of the cross-section, and introducing internal ribbing. The use of beams with a cross-section like a rectangle allows for high torsional stiffness with limited lateral stiffness. The prepared twin spar chassis is 2kg (23,5%) lighter than the steel frame, with the almost identical torsional rigidity of the frame.

The use of CFRP reinforced sections, due to the orthotropic nature of the CFRP, is another possibility to influence the rigidity of the chassis, even in the later stages of the product's life.

Two approaches to the construction of the welding jig were presented. Changes that can be made to the twin spar frame welding jig design, which has fewer components than a truss frame were described. The introduction of inserts in the headstock and the swingarm pivot can be considered as a way to adjust the geometry of the motorcycle and eliminate deviations created by the welding process.

Acknowledgment

References

Cossalter, V., (2006). *Motorcycle Dynamics,* 2nd ed. Lulu

Foale, T., (2002). *Motorcycle Handling and Chassis Design,* 1st ed. Spain: Tony Foale.

Khaled, T., (October 2014). Preheating, interpass and post-weld heat treatment requirements for welding low alloy steels. [Online]. Available: https://vdocuments.site/preheating-interpass-and-post-weld-heat-treatment-requirements-.html

Bocciolone, M., Cheli, F., Pezzola, M. and Vigano, R., (2005). Static and dynamic properties of a motorcycle frame: experimental and numerical approach. *Computational Methods and Experimental Measurements XII.* Malta, pp. 517-526.